HHS Public Access

Author manuscript

Pain. Author manuscript; available in PMC 2020 March 01.

Published in final edited form as:

Pain. 2019 March ; 160(3): 550–560. doi:10.1097/j.pain.0000000000001417.

Machine learning-based prediction of clinical pain using multimodal neuroimaging and autonomic metrics

Jeungchan Lee[#a], **Ishtiaq Mawla**[#a], **Jieun Kim**[a,b], **Marco L. Loggia**[a], **Ana Ortiz**[a], **Changjin Jung**[a,b], **Suk-Tak Chan**[a], **Jessica Gerber**[a], **Vincent J Schmithorst**[c], **Robert R. Edwards**[d], **Ajay D. Wasan**[e], **Chantal Berna**[f], **Jian Kong**[a,g], **Ted J. Kaptchuk**[h], **Randy L. Gollub**[a,g], **Bruce R. Rosen**[a], and **Vitaly Napadow**[a,2]

[a]Department of Radiology, Athinoula A. Martinos Center for Biomedical Imaging, Massachusetts General Hospital, Harvard Medical School, Charlestown, MA 02129, USA. [b]Division of Clinical Research, Korea Institute of Oriental Medicine, Daejeon 34054, Korea. [c]Department of Pediatric Radiology, Children's Hospital of Pittsburgh of UPMC and University of Pittsburgh School of Medicine, Pittsburgh, PA 15224, USA [d]Department of Anesthesiology, Perioperative and Pain Medicine, Brigham and Women's Hospital, Harvard Medical School, Boston, MA 02115, USA. [e]Department of Anesthesiology, Center for Pain Research, University of Pittsburgh, Pittsburgh, PA 15206, USA. [f]Pain Center, Department of Anesthesiology, Lausanne University Hospital (CHUV), Lausanne 1011, Switzerland. [g]Department of Psychiatry, Massachusetts General Hospital, Harvard Medical School, Boston, MA 02144, USA. [h]Program of Placebo Studies and the Therapeutic Encounter, Beth Israel Deaconess Medical Center, Harvard Medical School, Boston, MA 02215, USA.

[#] These authors contributed equally to this work.

1. Introduction

While self-report pain intensity ratings are the gold standard in clinical pain assessment, they are highly variable, inherently subjective in nature, and significantly influenced by multidimensional factors. The lack of objective biomarkers for pain has contributed to suboptimal chronic pain management (e.g., opioid public health crisis) [26]. Thus, research focused on the development of quantitative, objective biomarkers/predictors alongside self-report to aid diagnosis, estimate prognosis, and predict treatment efficacy is of increasing importance to combat chronic pain [24,30,32].

Growing consensus has suggested that altered central nervous system processing can support and maintain abnormal pain perception in chronic pain, implicating aberrant activity and connectivity of multiple functional brain networks, including default mode, salience, and

[2]Corresponding author: Vitaly Napadow, Address: Martinos Center for Biomedical Imaging, Building 149, suite 2301, Charlestown, MA 02129. Phone: +1 617-724-3402. Fax: +1-617-726-7422. vitaly@mgh.harvard.edu.

Author contributions: V.N., B.R.R., R.L.G., T.J.K., J.Kong, C.B., A.D.W., M.L.L., V.J.S., R.R.E., and J.Kim designed study. J.L., I.M., A.O., C.J., J.G., and S.T.C. performed research (acquisition of data). J.L., I.M., J.Kim, and V.N. analyzed data. J.L., I.M., and V.N. wrote the paper. Critical revision: All authors discussed the results and contributed to the final manuscript.

Competing interests: No conflict with respect to financial interests.

sensorimotor networks [3,20,21,43], as well as amplification of sensory input to the brain [28]. In addition, altered processing extends to the autonomic nervous system; a recent meta-analysis found that high frequency heart rate variability (HF_{HRV}) is reduced in chronic pain patients, suggesting that diminished parasympathetic modulation is also associated with chronic pain [35].

As brain imaging and autonomic data could potentially capture objective measures of the pain experience, multivariate machine-learning techniques have been gaining attention. Such techniques use “features” extracted from a set of clinically relevant data, allowing computer algorithms to “learn” from those features and form a predictive model. This model can then be applied to new datasets or individuals to diagnostically predict disease states or/and treatment efficacy [13]. Towards this goal, multivariate machine-learning techniques have used neuroimaging data to propose a brain signature for evoked experimental pain [39]. Neuroimaging-based pain prediction, however, has been in a discovery phase and mostly limited to discrimination of brain activity patterns contrasting noxious stimulus-evoked painful versus non-painful states in healthy, pain-free individuals [8,9,37] and estimation of experimental pain ratings [11,37,39]. A few prediction studies attempted to discriminate chronic pain patients from healthy controls [23,38], however, patients and controls can differ on much more than pain experience (e.g., mood, drug levels, etc.).To our knowledge, no study has attempted to classify clinical pain states (i.e. higher vs. lower clinical pain within an individual) or predict clinical pain ratings at the time of data acquisiton, which could provide greater clinical relevance. Moreover, previous studies have reported only modest accuracy and to our knowledge, no studies have tried to combine multimodal (e.g., central and autonomic) parameters to boost prediction of clinically relevant pain states using machine-learning techniques.

We built a multivariate machine-learning model that learns from central and autonomic features, and then classifies clinical pain states and predicts pain intensity. Importantly, in order to control clinical pain states, our approach modulated pain in chronic low back pain (cLBP) patients through physical maneuvers aimed to exacerbate their low back pain [21,43], thereby creating experimentally controlled lower and higher clinical pain states. Multimodal features included resting-state functional connectivity of the back representation in primary somatosensory cortex [17], whole-brain regional cerebral blood flow (rCBF) [21,27,43], and HF_{HRV} [35]. Our novel multimodal combinatorial machine-learning approach was then applied to classify and predict clinical pain intensity.

2. Methods

2.1. Patients

We enrolled 71 patients suffering from cLBP meeting Quebec Task Force Classification System categories I-II (i.e., patients were unlikely to have significant nerve root involvement, stenosis, or mechanical instability [2,22]) as confirmed by the study physician and/or review of medical records. All patients were screened with the following inclusion criteria for eligibility: (a) age between 18 and 60 years old with a diagnosis of chronic low back pain (cLBP, duration > 6 months) by physician, (b) average low back pain intensity > 4/10 during the past two weeks prior to consent (0: no pain, 10: most pain imaginable), (c)

fluent English, (d) ability to provoke or exacerbate clinical back pain by performing physical maneuvers. Eligibility was also assessed with the following exclusion criteria: (a) specific causes of back pain (such as cancer, fractures, spinal stenosis, and infections), (b) radicular pain extending below the knee, (c) complicated back problems such as prior back surgery, intent to undergo surgery at time of the study, and unresolved medical legal/disability/workers compensation claims in relation to cLBP, (d) major systemic or neuropsychiatric disease that might confound interpretation of results (e.g. severe fibromyalgia, rheumatoid arthritis, major psychiatric disorders, psychoses, seizure disorder, severe cardiorespiratory or nervous system diseases, etc.), (e) self-reported substance abuse disorder in the past two years, (f) contraindications to MRI scanning (e.g. cardiac pacemaker, metal implants, claustrophobia, and pregnancy), or (g) use of prescription opioids greater than 60 mg morphine equivalents per day or steroids for pain.

Successful maneuver-related pain increase and available data for all model parameters were limited to 53 patients, therefore we also limited classification, regression, and parameter evaluation and comparison to these 53 patients only (age = 37.37 ± 11.29 years old, mean ± SD, 33 female, pain duration=7.63 ± 7.42 years, range: 0.5 – 30). See Fig. S1 under Supplementary Materials for flowchart outlining data collected, excluded, and analyzed. All patients were informed of the entire experimental protocol and provided written informed consent. The IRB of Partners Human Research Committee approved this experimental protocol (2011P001364), and this study was performed in accordance with the principles of the Declaration of Helsinki (trial registration number at ClinicalTrials.gov: NCT01598974).

2.2. Study design and clinical pain exacerbation

In this study, back pain exacerbation maneuvers were implemented to increase the endogenous levels of clinical back pain in patients [18,21,43]. The maneuvers consisted of individualized dynamic physical procedures that exacerbated patient's clinical LBP intensity and were implemented based on discussions between patients and a trained experimenter during an initial behavioral session. Patients first listed usual activities that most exacerbated their back pain and performed certain repetitions of one or more of these typical back pain exacerbating maneuvers (such as toe touches, back arches, and facet-joint loading twists). Meanwhile, the experimenter kept detailed records of the number of repetitions, distance, depth, angle, and other respective metrics to allow for reproducibility of the maneuvers during MRI scan session. The experimenter also recorded pain ratings before and after maneuvers; based on our previous publications [18,21,43], the protocol aimed for at least 30% increase in subjective pain ratings without exceeding an intolerable pain level. The most common maneuvers employed by patients were toe touches (performed by 57% of patients), back arches (19%), and facet-joint loading twists (19%). A few patients could not exacerbate their back pain with typical maneuvers, hence we chose to have them perform a painful movement from their daily lives (e.g., one patient experienced intense pain while wearing socks, hence this set of actions were used repeatedly in a controlled manner to exacerbate back pain). The sole goal of this manipulation was to temporarily exacerbate clinical low back pain.

During the MRI scan session, all patients were scanned twice, once before and once after patients performed the low back pain exacerbation maneuvers (pre- and post-maneuver, respectively), to collect multimodal data associated with different (i.e., relatively lower and higher) clinical pain states. Neuroimaging data included resting-state functional magnetic resonance imaging (fMRI) with two approaches: (a) regional cerebral blood flow (rCBF) using Pseudo-Continuous Arterial Spin Labeling (PCASL) imaging and (b) functional connectivity of the primary somatosensory cortical representation of the back ($S1_{CONN}$) using Blood Oxygenation-Level Dependent (BOLD) imaging. PCASL is a noninvasive perfusion imaging method that provides absolute quantification of regional cerebral blood flow across the brain, and is ideal for capturing brain activity related to ongoing, slowly fluctuating clinical pain [43]. Additionally, a different functional imaging modality, BOLD, was used to investigate functional connectivity between the back representation in primary somatosensory cortex (S1) and the rest of the brain. Since physical maneuvers cause direct nociceptive processing in S1 and several studies have now implicated S1 in chronic pain [17,18,45], we evaluated whole-brain connectivity for this seed region, which was identified with a functional localizer using a separate BOLD fMRI scan (see Supplementary Materials, Section S1). Autonomic data included heart rate variability in the high-frequency range (HF_{HRV}), a marker for cardiovagal modulation. Thus, each of rCBF, $S1_{CONN,}$ and HF_{HRV} measures a unique dimension of central and autonomic processing for different clinical pain intensity states.

Patients rated clinical back pain intensity (0–100, 0: no pain, 100: most pain imaginable) before and following each fMRI scan run and maneuvers. An omnibus *F*-test was conducted on all post-maneuver clinical pain ratings, demonstrating no significant differences ($P = 0.19$), suggesting that maneuver-related clinical pain elevation was maintained throughout the post-maneuver period, until the end of the scanning session. Additionally, a separate omnibus *F*-test on all pre-maneuver clinical pain ratings showed no significant differences ($P = 0.43$), suggesting stability in ratings during the pre-maneuver period. Hence, average ratings of respective pre-maneuver and post-maneuver rating periods were used for subsequent analyses.

2.3. Acquisition of multimodal neuroimaging and autonomic parameters

All MRI data were collected at the Athinoula A. Martinos Center for Biomedical Imaging, Massachusetts General Hospital, using a 3.0T Siemens Skyra scanner (Siemens Medical, Germany) equipped with 32-channel head coil. Patients were asked to rest in a supine position inside the MRI scanner with their eyes open and head still during the data collection. A T1-weighted MP-RAGE pulse sequence (TR/TE = 2530/1.64 ms, flip angle = 7°, FOV = 256 × 256 mm, 176 axial slices, voxel size = 1 × 1 × 1 mm) was used to collect structural MRI data. Resting-state BOLD fMRI data were collected using a T2*-weighed gradient-echo BOLD EPI pulse sequence (TR/TE = 3000/30 ms, flip angle = 90°, FOV = 220 × 220 mm, 44 axial slices, voxel size = 2.62 × 2.62 × 3.12 mm, total acquisition time = 6 minutes). A Pseudo-Continuous Arterial Spin Labeling pulse sequence (PCASL, TR/TE = 3800/15 ms, labeling duration = 1500 ms, post-labeling delay = 1200 ms, flip angle = 90°, FOV = 256 × 256 mm, 25 axial slices, voxel size = 4 × 4 × 5 mm, total acquisition time = 6 minutes) was used to measure rCBF during ASL runs.

During the resting BOLD fMRI and ASL scan runs, physiological data including finger pulse and respiration were collected to calibrate artifacts from cardiovascular and respiratory movement from the fMRI data and to estimate autonomic, cardiovagal modulation during MRI scans associated with different pain states. Finger pulse was collected from the patient's left index finger using a piezoelectric pulse transducer (MLT1010 Non-Ferrous Transducer, ADInstruments, CO, USA), while respiration was measured using a custom-built MR-compatible pneumatic belt [6,17,19]. These physiological (cardiac pulse and respiration) signals were recorded at 500 Hz sampling frequency during the fMRI runs using a MRI-compatible system (MP150, Biopac Systems Inc.).

2.4. Preprocessing and assessment of multimodal neuroimaging and autonomic parameters

FMRI data were preprocessed using tools from SPM (Statistical Parametric Mapping, https://www.fil.ion.ucl.ac.uk/spm), FSL (FMRIB's Software Library, https://fsl.fmrib.ox.ac.uk/fsl/fslwiki/), AFNI (Analysis of Functional NeuroImages, https://afni.nimh.nih.gov), and FreeSurfer (https://surfer.nmr.mgh.harvard.edu) software packages.

Resting-state BOLD fMRI data were preprocessed with physiological artifact correction (3dretroicor, AFNI) [15], head motion correction (mcflirt, FSL), susceptibility-induced distortion correction (topup, FSL), and skull-stripping (bet, FSL). Additional artifacts were then removed using a GLM, modeling nuisance regressors for (*a*) heart rate and respiratory volume per time convolved with respective cardiorespiratory response functions [7,12], (*b*) white matter and cerebrospinal fluid data identified with the top five principal components using the COMPCOR algorithm [5,44] with FAST (FSL) tissue segmentation, (*c*) head motion correction parameters, and (*d*) a censoring confound matrix of head motion outliers (fsl_motion_outliers, FSL). The corrected data were co-registered to MNI space (bbregister, FreeSurfer), spatially smoothed (FWHM = 6 mm, fslmaths, FSL), and temporally high-pass filtered (cutoff frequency = 0.006 Hz, 3dBandpass, AFNI). For resting-state seed connectivity analysis, we used the S1 low back representation (see Supplementary Materials, Section S1), which was identified by a separate event-related functional localizer fMRI scan and evoked nociceptive stimulus. The S1 seed was created with a 4-mm radius sphere centered on the peak activation voxel within contralateral S1 (peak X/Y/Z location in MNI space = ±18/−38/72 mm). We created a bilateral seed ($S1_{back}$) by mirroring this sphere to the ipsilateral hemisphere, as for clinical pain, patients varied in low back pain laterality. Averaged fMRI signal from this $S1_{back}$ seed was used for seed connectivity analysis, and the parameter estimates from each patient were used for further analyses (i.e., $S1_{CONN}$) [17].

The PCASL data were used to estimate an rCBF map for each patient. Data were processed as follows: First, affine tag–control weighted motion correction was performed (batch_realign, ASLtbx, https://cfn.upenn.edu/~zewang/ASLtbx.php) [41,42], and these head motion realignment parameters were regressed out of the difference maps (rigid-body transformation-based MoCo, SPM) [41]. After high-pass filtering (cutoff frequency = 0.01 Hz), non-brain voxels were removed from the data (BET, FSL) [31]. Additionally, physiological noise (driven by cardiovascular fluctuation) was regressed out using a GLM with 6 principal components from anatomically defined cerebrospinal fluid (CSF) and white

matter (WM) regions using the COMPCOR algorithm [5,44]. Tag and control images were then subtracted, and the average of subtracted pairs was divided by the average of control images to obtain a percent change in rCBF. The percent change maps were converted to absolute values (mm/100 g of tissue/min) [42]. These rCBF maps were co-registered to individual structural images (bbregister, FreeSurfer) [16], followed by non-linear transformation into MNI152 common space (FNIRT, FSL). Finally, whole brain rCBF normalization and spatial smoothing (FWHM = 8 mm) were performed [40].

Cardiac pulse pressure data collected during ASL scan runs, were used for HRV analysis to estimate cardiovagal modulation associated with different (i.e., low and high) clinical pain states. In-house scripts (MATLAB 8.3, MathWorks) were used to annotate the finger pulse signal. Commonly available HRV analysis software (HRV standard, Kubios) was used to calculate HRV parameters including high frequency (HF) power (i.e., HF_{HRV}), which is a well-known marker for cardiovagal modulation [1,35].

2.5. Classification of clinical pain states using a support vector machine algorithm

For classification of clinical pain states (i.e., between relatively lower and higher clinical pain), a supervised support vector machine (SVM, scikit-learn 0.18.1, https://scikit-learn.org/stable/) with linear kernel was used, as this algorithm is known to have high accuracy and easy interpretability [25]. Briefly, the SVM algorithm segregates two classes (relatively lower pain vs. higher pain, in this case) of data in feature space by finding an optimal hyperplane/decision boundary that maximally separates them. As our multimodal data were collected at two time points for each patient (i.e., before and after physical maneuvers), and variability existed in baseline clinical pain level for each patient, we used a paired-SVM approach wherein within-patient differences in the pre- and post-maneuver data (i.e., change in pain) were emphasized, and baseline pain levels across patients were accounted for (Fig. 1A). The paired-SVM classifier discriminated ‘pre – post’ versus ‘post – pre’ parameter differences (Fig. 1B), a procedure that has been utilized in past brain imaging research to discriminate state differences between two time points [33]. Paired-SVM classification was applied for each parameter (i.e., $S1_{CONN}$, rCBF, and HF_{HRV}) independently, yielding SVM classification weights (i.e., contribution of each feature/voxel to the classification) and decision responses (i.e., the dot product between SVM weights and feature/voxel values for each modality in each patient, where the classification is determined by the sign of these response values) (Fig. 1C) [39]. Results of classification for each modality (i.e., decision responses) were then used for a combined multimodal parameter classification in an attempt to bolster prediction compared to single-modality prediction models [23].

2.6. Prediction of clinical pain intensity using a support vector regression algorithm

Next, we sought to predict clinical pain intensity obtained at the time of data acquisition in a between-patients manner using a linear support vector regression (SVR) algorithm. Briefly, linear SVR tries to find a linear function that fits all continuous data points (clinical pain intensity ratings, in this case), with minimized error. SVR is appropriate for predicting continuous variables, as opposed to SVM, which has the goal of separating classes of data.

In order to prepare the data for SVR analysis, each clinical pain rating was considered an independent sample; in other words, data belonging to an individual patient were used independently in an unpaired manner. This procedure was done to obtain an effective $N = 106$ for clinical pain ratings and corresponding multimodal features, allowing us to break-up and allocate the samples into separate training ($N = 53$) and testing ($N = 53$) datasets. The training dataset allowed for creation of the SVR model and the testing dataset allowed for validation of the model.

The allocation of clinical pain ratings into training and testing datasets was done through randomization of these 106 clinical pain ratings (as illustrated in Fig. 2A). After randomization, the distribution of clinical pain intensity was equalized and the dynamic range was no longer discrepant (see Results, section 3.3). Furthermore, we posited that the randomization potentially mitigated any bias of experimental design, i.e. for the SVM, the lower pain state (timepoint 1) always occurred prior to the higher pain state (timepoint 2) (pre-maneuver always occurred before post-maneuver). Randomization allowed for the training dataset to include an equal number of cases from both timepoint 1 and timepoint 2 (same for the testing dataset), hence accounting for any potential order effects between a training and testing dataset.

After allocation into training and testing, each clinical pain intensity rating and the corresponding multimodal features (rCBF, $S1_{CONN}$, and HF_{HRV}) for each patient were used to calculate decision responses (Fig. 2B), representing the degree to which features corresponding to each clinical pain intensity loads on to the clinical pain state SVM model. In other words, the decision response links the SVM model's confidence of discriminating lower versus higher pain states with raw features corresponding to a range of clinical pain ratings (**see footnote**†).

The decision responses and their corresponding clinical pain intensity ratings in the training dataset were then used to train/build the SVR model (Fig. 2C, left panel). Next, the trained SVR model was evaluated for consistency using independent multimodal SVM decision responses in the testing dataset with corresponding pain ratings, and the predicted pain ratings were compared with true pain ratings reported by the patients (Fig. 2C, right panel).

2.7. Statistical analysis

After the within-patient classification of pain intensity states using paired-SVM, leave-one-patient-out cross-validation was performed to evaluate classification performance (i.e., accuracy, sensitivity, specificity, precision and area under the curve, AUC). For the paired-SVM approach, sensitivity, specificity, and precision are identical to the accuracy due to the paired characteristics (i.e., number of True Positives (TP) = True Negatives (TN), False Positives (FP) = False Negatives (FN)). Permutation analysis was also performed ($N = 5000$,

†To elaborate this further, let's say that a particular voxel in $S1_{CONN}$ SVM map shows a high positive weight (i.e. highly confident and robust discrimination of post – pre >> pre – post); the dot product of this SVM weight with $S1_{CONN}$ voxel intensity corresponding to a particular clinical pain intensity will produce a positive decision response with a high magnitude. Similar procedures have been used in past research [23], where weights from a previously created model of experimental heat pain [39] was applied (as a dot product) to brain features from assessment of experimental mechanical pain in fibromyalgia patients. The outcome of the computation was the degree to which brain activity to mechanical pain in fibromyalgia loaded on to the generalizable experimental heat pain model, allowing for inferences of hypersensitivity to be made [23].

$P < 0.01$) to identify the significant features contributing to the classification of different pain intensity states, and to calculate significance of classification measures by comparison with those from a random classifier.

For the between-patients SVR analysis, the correlation coefficient (i.e., Pearson's r) and root mean square error (RMSE) between true pain ratings provided by patients (i.e., true LBP) and predicted pain ratings provided by the algorithm (i.e., predicted LBP) was calculated to assess prediction model performance, and significance was tested with permutation analysis ($N = 5000$, $P < 0.01$). For a case of perfect prediction (i.e., predicted pain = true pain), the Pearson's r value would be 1 and RMSE would be 0.

3. Results

3.1. Higher clinical pain elicited by physical maneuvers

Patients suffering from chronic low back pain (cLBP, $N = 53$ used in final analyses, Table 1 and Supplementary Materials, Fig. S1) were recruited to perform physical maneuvers that exacerbated back pain intensity during an fMRI session. Both brain and autonomic data were collected at two different clinical pain states for each patient (i.e., pre- and post-physical maneuvers). Patients reported increased average LBP intensity following physical maneuvers (change in LBP: +23.6 ± 12.3/100, mean ± SD, $P < 0.00001$, pre-maneuver LBP: 31.6 ± 19.0, post-maneuver LBP: 55.2 ± 18.9, 0–100 numerical rating scale, where 0 was "no pain" and 100 was "most pain imaginable") (Fig. 3A). Variability in baseline clinical pain level (i.e., pre-maneuvers) was considerable and ranged from 0 to 72.5 out of 100 (Fig. 3B), supporting our paired-SVM approach for within-subject evaluation.

3.2. Within-patient classification of low and high clinical pain states

Multivariate machine learning-based classification was applied to predict clinical pain intensity states (i.e., relatively higher versus lower clinical pain states, as modulated by physical maneuvers in cLBP patients), using combinations of multimodal neuroimaging (brain) and autonomic outflow parameters. Patients responded to maneuvers with significant decrease in HF_{HRV} (change: −0.29 ± 0.47 log(ms^2), paired t-test $P < 0.001$, pre: 6.02 ± 1.15, post: 5.73 ± 1.21).

A supervised paired-SVM algorithm was used to learn from the aforementioned parameters (rCBF, $S1_{CONN}$, HF_{HRV}) (Fig. 1) and to classify relatively lower and higher pain states. Paired-SVM classification found that, independently, all three parameters significantly contributed to the within-patient classification between pain intensity states (rCBF: accuracy = 81.13%, AUC = 0.90, TP/TN/FP/FN = 43/10/10/43; $S1_{CONN}$: 79.24%, 0.85, 42/11/11/42; HF_{HRV}: 67.92%, 0.81, 36/17/17/36). The voxelwise paired-SVM weight map for rCBF classified higher vs. lower clinical pain states through increased cerebral blood flow to several subcortical and cortical structures including thalamus, and prefrontal and posterior cingulate cortices, and decreased flow to non-back representation subregions of S1 (i.e., outside the putative location of the somatotopic representation of the back) (Fig. 4A, and Supplementary Materials, Table S1). For $S1_{CONN}$, the paired-SVM weight map classified higher vs. lower clinical pain through increased $S1_{back}$ connectivity to frontoinsular cortex,

and decreased connectivity to medial prefrontal cortex and other non-back representation subregions of S1/M1 cortices (Fig. 4B, and Supplementary Materials, Table S2).

Moreover, combining multimodal parameters (rCBF + $S1_{CONN}$ + HF_{HRV}) (Fig. 1) produced the best classification performance (accuracy = 92.45%, AUC = 0.97, TP/FP/FN/TN = 49/4/4/49) compared to the classification with individual parameters as noted above (Fig. 5). For this combined model, all three multimodal parameters significantly contributed ($S1_{CONN}$ and rCBF: $P < 0.001$, and HF_{HRV}: $P = 0.007$) to the classification.

As head motion may confound neuroimaging findings, we explored the relationship between head motion and within-patient pain state classification. Head motion showed no significant contribution to discriminate relatively lower versus higher clinical pain intensity states ($P = 0.31$) (Supplementary Materials, Section S2).

3.3. Between-patient prediction of clinical pain intensity ratings

Another goal of our analysis was to form a model that can directly predict clinical pain intensity ratings across patients through the introduction of independent training and testing datasets using multimodal parameters. Hence, we conducted a linear SVR analysis, which is optimized for the prediction of continuous variables such as clinical pain ratings (Fig. 2). Data from different patients and different time points, including corresponding clinical pain intensity ratings, were randomized into separate training ($N = 53$) and testing ($N = 53$) datasets, allowing for the range of clinical pain intensity values to be equalized (Fig. 2A). After randomization, the distribution of clinical pain intensity was equalized (clinical pain intensity range: training set = 0–92.8/100, testing set = 0–86.7; clinical pain intensity: training set = 43.38 ± 23.76/100, testing set = 43.45 ± 20.90, $P = 0.98$).

Combining all three multimodal parameters (i.e., decision responses of $S1_{CONN}$, rCBF, and HF_{HRV}) for prediction of pain intensity ratings demonstrated significant performance in terms of predicted versus true clinical pain intensity ratings for both the independent training (Pearson's $r = 0.52$, RMSE = 20.51) and testing ($r = 0.63$, $P = 0.02$, RMSE = 16.69, $P < 0.001$, Fig. 6) datasets. For this combined model, only the $S1_{CONN}$ parameter significantly contributed ($S1_{CONN}$: $P = 0.002$, rCBF: $P = 0.31$, HF_{HRV}: $P = 0.41$) for the prediction.

Head motion did not significantly predict clinical pain intensity ratings ($P = 0.30$). In fact, when head motion was included in the prediction model as a fourth parameter, the correlation between true LBP and predicted LBP did not show much change ($r = 0.63$) compared to our three-parameter model where head motion was not included ($r = 0.63$) (Supplementary Materials, Section S2).

In order to explore the degree to which SVR accuracy was driven by maneuver-induced changes, we examined two other, new SVR models which did not randomize or reallocate data (i.e. would not be driven by a maneuver effect wherein datasets contained some patients at pre-maneuver and some at post-maneuver): (a) SVR with pre-maneuver data only, (b) SVR with post-maneuver data only. Thus, these SVR models allowed us to test if SVM weights (built from maneuver-induced changes) can be used to predict between-subject pain ratings in a dataset with consistent timing relative to physical maneuver performance.

Results showed that while the SVR performed with pre-maneuver data only yielded a poor correlation ($r = -0.07$, $P = 0.63$) between actual and predicted pain ratings, the SVR performed with post-maneuver data only yielded a much better correlation between actual and predicted pain ratings ($r = 0.42$, $P = 0.002$).

4. Discussion

While pain is inherently a subjective self-reported experience, there is growing need for objective biomarkers for pain. We address a significant gap in the clinical pain research field by introducing and evaluating candidate predictive, combinatorial biomarkers for clinical pain intensity. Multimodal brain and autonomic physiology data were evaluated with machine learning-based prediction modeling in cLBP patients. Individualized physical maneuvers were successfully implemented to exacerbate clinical back pain for post-maneuver brain imaging scan runs in the majority of cLBP patients (87%, 62 out of 71 patients). For these patients, maneuvers produced an average increase of 74.8% in clinical pain, allowing us to evaluate patients in a relatively lower versus higher clinical pain state. When combined, multimodal parameters ($S1_{CONN}$, rCBF and HF_{HRV}) produced a synergistic effect, resulting in successful within-patient classification between relatively lower and higher clinical pain intensity states with high accuracy. Moreover, this model was successfully applied to predict between-patient clinical pain ratings with minimal prediction model overfitting and with independent training and testing datasets [24].

Each putative biomarker targeted a unique physiological dimension of central and autonomic processing supporting pain. For instance, rCBF is obtained from ASL fMRI, and captures slowly varying state changes in activity across the brain that may be linked to pain exacerbation. $S1_{CONN}$ was obtained from BOLD fMRI data and captured the temporal coherence (whole-brain connectivity) of the S1 representation of the low back, which is the primary encoding node for afferent nociceptive information from the involved body region. For these brain imaging data, we used a whole-brain predictive model, which bolstered our predictive capacity [45]. Finally, HF_{HRV} captures the altered autonomic outflow associated with change in clinical pain perception. Importantly, combining these multimodal putative biomarkers produced a synergistic effect for clinical pain prediction, both within and between cLBP patients.

Classification was strongly influenced by the brain imaging features, and the SVM weighting maps inform the brain circuitry that directly supports higher clinical pain intensity. For instance, the rCBF parameter weighting map encompassed positive predictive weights in subcortical regions such as the thalamus, and cortical pain-processing regions such as the prefrontal cortex and ventral posterior cingulate cortex. Regions such as thalamus are known to process nociception and pain salience [14], while prefrontal cortex has been strongly linked to clinical pain perception [4], and posterior cingulate has been recently implicated in pain catastrophizing [19]. For $S1_{CONN}$, increased communication between the low back representation of S1 and frontoinsular cortex (a key hub for salience/affect processing [17]) is a significant feature for classification. In turn, negative predictive weighting was evident for non-back S1 representation in the rCBF map, and both non-back S1 subregions and medial prefrontal cortex in the $S1_{CONN}$ map. Interestingly, our prior

analyses have also demonstrated reduced connectivity between S1 subregions in chronic pain patients [17]. Collectively, these positive and negative predictive weighting regions are key nodes of known brain networks implicated in the affective, cognitive, and sensory multidimensional experience of pain – i.e. salience, default mode, and sensorimotor networks.

While our results showed less robust classification accuracy for the autonomic HF_{HRV} metric, decreased cardiovagal modulation did significantly contribute to prediction of relatively higher versus lower clinical pain states. The primary reason behind low accuracy for the HF_{HRV} metric could be due to the single-feature nature of this metric, leading to a fit of the decision boundary in a unidimensional feature space (as shown in Fig. 1B). In contrast, the brain imaging metrics contained thousands of features/voxels. Indeed, future research should incorporate several autonomic metrics (both time-domain and frequency-domain cardiac information, galvanic skin response, pupilometry) to allow for a multidimensional feature space and better model performance.

To our knowledge, the analyses in this current study represents the first use of multimodal central and autonomic data to directly predict clinical pain states. One recent promising study used multimodal task-evoked brain imaging data to discriminate between fibromyalgia patients and healthy controls [23]. However, fibromyalgia patients and healthy adults differ on much more than just the pain experience (e.g., mood, cognitive task performance, etc.), and this study linked model prediction to pain intensity assessed at a different time point (an hour prior to brain imaging acquisiton). Our study significantly extends such previous work by building a multimodal predictive model that provides diagnostic and clinical utility by directly predicting concurrent clinical pain states.

The use of a within-patient model in our study through pain exacerbation maneuvers mitigates inter-individual differences in how different patients interpret and use a numerical pain rating scale. Furthermore, extension of these multimodal data to a between-patient analysis using training and testing datasets allow prediction of clinical pain intensity across different patients. The between-patient SVR was conducted through randomized 50–50% allocation of pre- and post-maneuver data into respective training and testing datasets, which mitigates effects such as passage of time, as the lower-pain state always occurred prior to the higher-pain state. When the SVR was performed without this randomized allocation, i.e. SVR performed with pre-maneuver data only and a separate SVR performed with post-maneuver data only, the pre-maneuver data SVR demonstrated poor performance ($r = -0.07$), whereas the post-maneuver data SVR demonstrated significant actual-to-predicted pain correlation ($r = 0.42$). Our interpretation is that pre-maneuver ratings may have been influenced by a broad array of factors leading to substantial differences in how individuals use the 0–100 pain scale we presented to them. On the other hand, after completing the maneuvers, which increased their pain, all cLBP patients had a consistent anchor as reference for how to rate their back pain – an explicit, physical maneuver-exacerbated back pain. This effectively normalized how patients used the 0–100 pain scale post-maneuvers, leading to better prediction of clinical pain ratings by our SVR model, which was created using a maneuver-evoked SVM design. Further testing on future, independent samples would of course be needed to assess generalizability of this SVR model, but providing this

anchor for ratings seems to be beneficial for prediction, and is in line with previous studies suggesting that clinical pain rating fidelity can be enhanced with training in how to consistently use pain scales, for example by applying evoked pain stimuli as anchors [36].

Data fusion techniques for multimodal brain imaging data take advantage of combining unique aspects of each data modality's contribution to enhance prediction. However, the use of such multimodal combinatorial prediction techniques has remained limited [10]. We demonstrated synergistic performance when parameters from different modalities were combined. Our multimodal approach could be further extended to include other brain imaging (e.g., structural MRI, diffusion tensor imaging, positron emission tomography, chemical shift imaging, magnetoencephalography, and electroencephalography), physiological/autonomic activity (including time-domain and other frequency-domain metrics of HRV, galvanic skin response, pupilometry), behavioral (e.g., facial expression and body gesture), mood/affect parameters (e.g., state-based pain catastrophizing and anxiety), and quantitative sensory testing (QST) measures, as well as experimental tasks related to different (e.g., sensory, affective, cognitive) aspects of pain.

Our research is in line with increased interest in predictive modeling with brain-based biomarkers [45]. The clinical pain classification and prediction model created in this study could eventually lead to applications in clinical practice, and could help predict pain intensity for clinical settings without the presence of patient-reported ratings (e.g., non-communicative patients). Furthermore, combining several non-neuroimaging parameters for prediction could lead to a more cost-effective and quicker approach to pain prediction in clinical practice. However, this field is still nascent – the current consensus around such multivariate predictive models is that they should not be used in lieu of subjective clinical pain ratings, but rather in conjunction with and supporting clinical pain ratings. Such neuroimaging approaches can be used to understand the underlying mechanisms of clinical pain [13]. We hope that the model presented in this study will lead to future research to create well-validated predictive models from larger samples and multimodal features, eventually working towards clinical application.

Limitations to our study should also be noted. For instance, since successful maneuver-related pain increase and available data for all model parameters were limited to 53 patients, we also limited classification, regression, and parameter evaluation and comparison to these 53 patients only. Future applications should extend our predictive model to multiple sampling visits within a longitudinal trial framework. In addition, we did not include any control conditions (e.g., healthy controls performing maneuvers). However, our previous study [43] found that only chronic back pain patients (and not healthy controls performing the same maneuvers) showed any changes in rCBF maps between the pre- and post-maneuver periods. Hence we wanted to allocate resources toward larger sample size for this current study. A further limitation is that we used pulse signal from subjects' fingers instead of ECG to compute HF_{HRV}. This finger pulse signal was used as it was not contaminated by MRI scanner noise. Finger pulse-based HF_{HRV} is not as commonly used or evidence-supported as ECG, however, our group has successfully used pulse-based frequency-domain metrics in several recently published studies [29].

In conclusion, our machine-learning approach with a clinical pain exacerbation model found synergistic effects of using multimodal brain and autonomic markers in classification of clinical pain states and prediction of pain intensity. If the model is generalized across different chronic pain populations and different contexts, this pain signature could have great promise for pain assessment in non-communicative patients, and identification of objective pain endophenotypes [34] that can be used in future longitudinal research aimed at discovery of new approaches to combat chronic pain [13].

Supplementary Material

Refer to Web version on PubMed Central for supplementary material.

Acknowledgements

Funding information: This project was supported by the National Institutes of Health, National Center for Complementary and Integrative Health (P01-AT006663, R01-AT007550, R61-AT009306), the National Institute of Arthritis and Musculoskeletal and Skin Diseases (R01-AR064367), the National Center for Research Resources (P41RR14075, S10RR021110, S10RR023043), and the National Institute of Neurological Disorders and Stroke (R01 NS095937–01A1, R21 NS087472–01A1, R01 NS094306–01A1). Support was also generously provided by the Korea Institute of Oriental Medicine (K18051).

References

[1]. Heart rate variability. Standards of measurement, physiological interpretation, and clinical use. Task Force of the European Society of Cardiology and the North American Society of Pacing and Electrophysiology. European heart journal 1996;17(3):354–381. [PubMed: 8737210]

[2]. Abenhaim L, Rossignol M, Valat JP, Nordin M, Avouac B, Blotman F, Charlot J, Dreiser RL, Legrand E, Rozenberg S, Vautravers P. The role of activity in the therapeutic management of back pain. Report of the International Paris Task Force on Back Pain. Spine (Phila Pa 1976) 2000;25(4 Suppl):1S–33S. [PubMed: 10707404]

[3]. Baliki MN, Baria AT, Apkarian AV. The cortical rhythms of chronic back pain. The Journal of neuroscience : the official journal of the Society for Neuroscience 2011;31(39):13981–13990. [PubMed: 21957259]

[4]. Baliki MN, Chialvo DR, Geha PY, Levy RM, Harden RN, Parrish TB, Apkarian AV. Chronic pain and the emotional brain: specific brain activity associated with spontaneous fluctuations of intensity of chronic back pain. The Journal of neuroscience : the official journal of the Society for Neuroscience 2006;26(47):12165–12173. [PubMed: 17122041]

[5]. Behzadi Y, Restom K, Liau J, Liu TT. A component based noise correction method (CompCor) for BOLD and perfusion based fMRI. Neuroimage 2007;37(1):90–101. [PubMed: 17560126]

[6]. Binks AP, Banzett RB, Duvivier C. An inexpensive, MRI compatible device to measure tidal volume from chest-wall circumference. Physiological measurement 2007;28(2):149–159. [PubMed: 17237587]

[7]. Birn RM, Smith MA, Jones TB, Bandettini PA. The respiration response function: the temporal dynamics of fMRI signal fluctuations related to changes in respiration. Neuroimage 2008;40(2): 644–654. [PubMed: 18234517]

[8]. Brodersen KH, Wiech K, Lomakina EI, Lin CS, Buhmann JM, Bingel U, Ploner M, Stephan KE, Tracey I. Decoding the perception of pain from fMRI using multivariate pattern analysis. Neuroimage 2012;63(3):1162–1170. [PubMed: 22922369]

[9]. Brown JE, Chatterjee N, Younger J, Mackey S. Towards a physiology-based measure of pain: patterns of human brain activity distinguish painful from non-painful thermal stimulation. PloS one 2011;6(9):e24124. [PubMed: 21931652]

[10]. Calhoun VD, Sui J. Multimodal fusion of brain imaging data: A key to finding the missing link(s) in complex mental illness. Biological psychiatry Cognitive neuroscience and neuroimaging 2016;1(3):230–244. [PubMed: 27347565]

[11]. Cecchi GA, Huang L, Hashmi JA, Baliki M, Centeno MV, Rish I, Apkarian AV. Predictive dynamics of human pain perception. PLoS Comput Biol 2012;8(10):e1002719. [PubMed: 23133342]

[12]. Chang C, Cunningham JP, Glover GH. Influence of heart rate on the BOLD signal: the cardiac response function. Neuroimage 2009;44(3):857–869. [PubMed: 18951982]

[13]. Davis KD, Flor H, Greely HT, Iannetti GD, Mackey S, Ploner M, Pustilnik A, Tracey I, Treede RD, Wager TD. Brain imaging tests for chronic pain: medical, legal and ethical issues and recommendations. Nat Rev Neurol 2017;13(10):624–638. [PubMed: 28884750]

[14]. Downar J, Mikulis DJ, Davis KD. Neural correlates of the prolonged salience of painful stimulation. Neuroimage 2003;20(3):1540–1551. [PubMed: 14642466]

[15]. Glover GH, Li TQ, Ress D. Image-based method for retrospective correction of physiological motion effects in fMRI: RETROICOR. Magnetic resonance in medicine 2000;44(1):162–167. [PubMed: 10893535]

[16]. Greve DN, Fischl B. Accurate and robust brain image alignment using boundary-based registration. Neuroimage 2009;48(1):63–72. [PubMed: 19573611]

[17]. Kim J, Loggia ML, Cahalan CM, Harris RE, Beissner FDPN, Garcia RG, Kim H, Wasan AD, Edwards RR, Napadow V. The somatosensory link in fibromyalgia: functional connectivity of the primary somatosensory cortex is altered by sustained pain and is associated with clinical/autonomic dysfunction. Arthritis & rheumatology 2015;67(5):1395–1405. [PubMed: 25622796]

[18]. Kong J, Spaeth RB, Wey HY, Cheetham A, Cook AH, Jensen K, Tan Y, Liu H, Wang D, Loggia ML, Napadow V, Smoller JW, Wasan AD, Gollub RL. S1 is associated with chronic low back pain: a functional and structural MRI study. Mol Pain 2013;9:43. [PubMed: 23965184]

[19]. Lee J, Protsenko E, Lazaridou A, Franceschelli O, Ellingsen DM, Mawla I, Isenburg K, Berry MP, Galenkamp L, Loggia ML, Wasan AD, Edwards RR, Napadow V. Encoding of self-referential pain catastrophizing in posterior cingulate cortex in fibromyalgia. Arthritis & rheumatology 2018.

[20]. Loggia ML, Berna C, Kim J, Cahalan CM, Martel MO, Gollub RL, Wasan AD, Napadow V, Edwards RR. The lateral prefrontal cortex mediates the hyperalgesic effects of negative cognitions in chronic pain patients. J Pain 2015;16(8):692–699. [PubMed: 25937162]

[21]. Loggia ML, Kim J, Gollub RL, Vangel MG, Kirsch I, Kong J, Wasan AD, Napadow V. Default mode network connectivity encodes clinical pain: an arterial spin labeling study. Pain 2013;154(1):24–33. [PubMed: 23111164]

[22]. Loisel P, Vachon B, Lemaire J, Durand MJ, Poitras S, Stock S, Tremblay C. Discriminative and predictive validity assessment of the quebec task force classification. Spine (Phila Pa 1976) 2002;27(8):851–857. [PubMed: 11935108]

[23]. Lopez-Sola M, Woo CW, Pujol J, Deus J, Harrison BJ, Monfort J, Wager TD. Towards a neurophysiological signature for fibromyalgia. Pain 2017;158(1):34–47. [PubMed: 27583567]

[24]. Lotsch J, Ultsch A. Machine learning in pain research. Pain 2018;159(4):623–630. [PubMed: 29194126]

[25]. Naselaris T, Kay KN, Nishimoto S, Gallant JL. Encoding and decoding in fMRI. Neuroimage 2011;56(2):400–410. [PubMed: 20691790]

[26]. National Academies of Sciences Engineering and Medicine Committee on Pain Management and Regulatory Strategies to Address Prescription Opioid Abuse. Pain Management and the Opioid Epidemic: Balancing Societal and Individual Benefits and Risks of Prescription Opioid Use. Washington (DC): National Academies Press (US), 2017.

[27]. O'Muircheartaigh J, Marquand A, Hodkinson DJ, Krause K, Khawaja N, Renton TF, Huggins JP, Vennart W, Williams SC, Howard MA. Multivariate decoding of cerebral blood flow measures in a clinical model of on-going postsurgical pain. Human brain mapping 2015;36(2):633–642. [PubMed: 25307488]

[28]. Phillips K, Clauw DJ. Central pain mechanisms in chronic pain states--maybe it is all in their head. Best practice & research Clinical rheumatology 2011;25(2):141–154. [PubMed: 22094191]

[29]. Sclocco R, Beissner F, Desbordes G, Polimeni JR, Wald LL, Kettner NW, Kim J, Garcia RG, Renvall V, Bianchi AM, Cerutti S, Napadow V, Barbieri R. Neuroimaging brainstem circuitry supporting cardiovagal response to pain: a combined heart rate variability/ultrahigh-field (7 T) functional magnetic resonance imaging study. Philos Trans A Math Phys Eng Sci 2016;374(2067).

[30]. Skolnick P, Volkow ND. Re-energizing the Development of Pain Therapeutics in Light of the Opioid Epidemic. Neuron 2016;92(2):294–297. [PubMed: 27764663]

[31]. Smith SM. Fast robust automated brain extraction. Human brain mapping 2002;17(3):143–155. [PubMed: 12391568]

[32]. Smith SM, Dworkin RH, Turk DC, Baron R, Polydefkis M, Tracey I, Borsook D, Edwards RR, Harris RE, Wager TD, Arendt-Nielsen L, Burke LB, Carr DB, Chappell A, Farrar JT, Freeman R, Gilron I, Goli V, Haeussler J, Jensen T, Katz NP, Kent J, Kopecky EA, Lee DA, Maixner W, Markman JD, McArthur JC, McDermott MP, Parvathenani L, Raja SN, Rappaport BA, Rice ASC, Rowbotham MC, Tobias JK, Wasan AD, Witter J. The Potential Role of Sensory Testing, Skin Biopsy, and Functional Brain Imaging as Biomarkers in Chronic Pain Clinical Trials: IMMPACT Considerations. The journal of pain : official journal of the American Pain Society 2017;18(7):757–777. [PubMed: 28254585]

[33]. Sripada CS, Kessler D, Welsh R, Angstadt M, Liberzon I, Phan KL, Scott C. Distributed effects of methylphenidate on the network structure of the resting brain: a connectomic pattern classification analysis. Neuroimage 2013;81:213–221. [PubMed: 23684862]

[34]. Tracey I Can neuroimaging studies identify pain endophenotypes in humans? Nat Rev Neurol 2011;7(3):173–181. [PubMed: 21304481]

[35]. Tracy LM, Ioannou L, Baker KS, Gibson SJ, Georgiou-Karistianis N, Giummarra MJ. Meta-analytic evidence for decreased heart rate variability in chronic pain implicating parasympathetic nervous system dysregulation. Pain 2016;157(1):7–29. [PubMed: 26431423]

[36]. Treister R, Lawal OD, Shecter JD, Khurana N, Bothmer J, Field M, Harte SE, Kruger GH, Katz NP. Accurate pain reporting training diminishes the placebo response: Results from a randomised, double-blind, crossover trial. PloS one 2018;13(5):e0197844. [PubMed: 29795665]

[37]. Tu Y, Tan A, Bai Y, Hung YS, Zhang Z. Decoding Subjective Intensity of Nociceptive Pain from Pre-stimulus and Post-stimulus Brain Activities. Front Comput Neurosci 2016;10:32. [PubMed: 27148029]

[38]. Ung H, Brown JE, Johnson KA, Younger J, Hush J, Mackey S. Multivariate classification of structural MRI data detects chronic low back pain. Cerebral cortex (New York, NY : 1991) 2014;24(4):1037–1044.

[39]. Wager TD, Atlas LY, Lindquist MA, Roy M, Woo CW, Kross E. An fMRI-based neurologic signature of physical pain. N Engl J Med 2013;368(15):1388–1397. [PubMed: 23574118]

[40]. Wang J, Wang Z, Aguirre GK, Detre JA. To smooth or not to smooth? ROC analysis of perfusion fMRI data. Magnetic resonance imaging 2005;23(1):75–81. [PubMed: 15733791]

[41]. Wang Z Improving cerebral blood flow quantification for arterial spin labeled perfusion MRI by removing residual motion artifacts and global signal fluctuations. Magnetic resonance imaging 2012;30(10):1409–1415. [PubMed: 22789842]

[42]. Wang Z, Aguirre GK, Rao H, Wang J, Fernandez-Seara MA, Childress AR, Detre JA. Empirical optimization of ASL data analysis using an ASL data processing toolbox: ASLtbx. Magnetic resonance imaging 2008;26(2):261–269. [PubMed: 17826940]

[43]. Wasan AD, Loggia ML, Chen LQ, Napadow V, Kong J, Gollub RL. Neural correlates of chronic low back pain measured by arterial spin labeling. Anesthesiology 2011;115(2):364–374. [PubMed: 21720241]

[44]. Whitfield-Gabrieli S, Nieto-Castanon A. Conn: a functional connectivity toolbox for correlated and anticorrelated brain networks. Brain connectivity 2012;2(3):125–141. [PubMed: 22642651]

[45]. Woo CW, Chang LJ, Lindquist MA, Wager TD. Building better biomarkers: brain models in translational neuroimaging. Nat Neurosci 2017;20(3):365–377. [PubMed: 28230847]

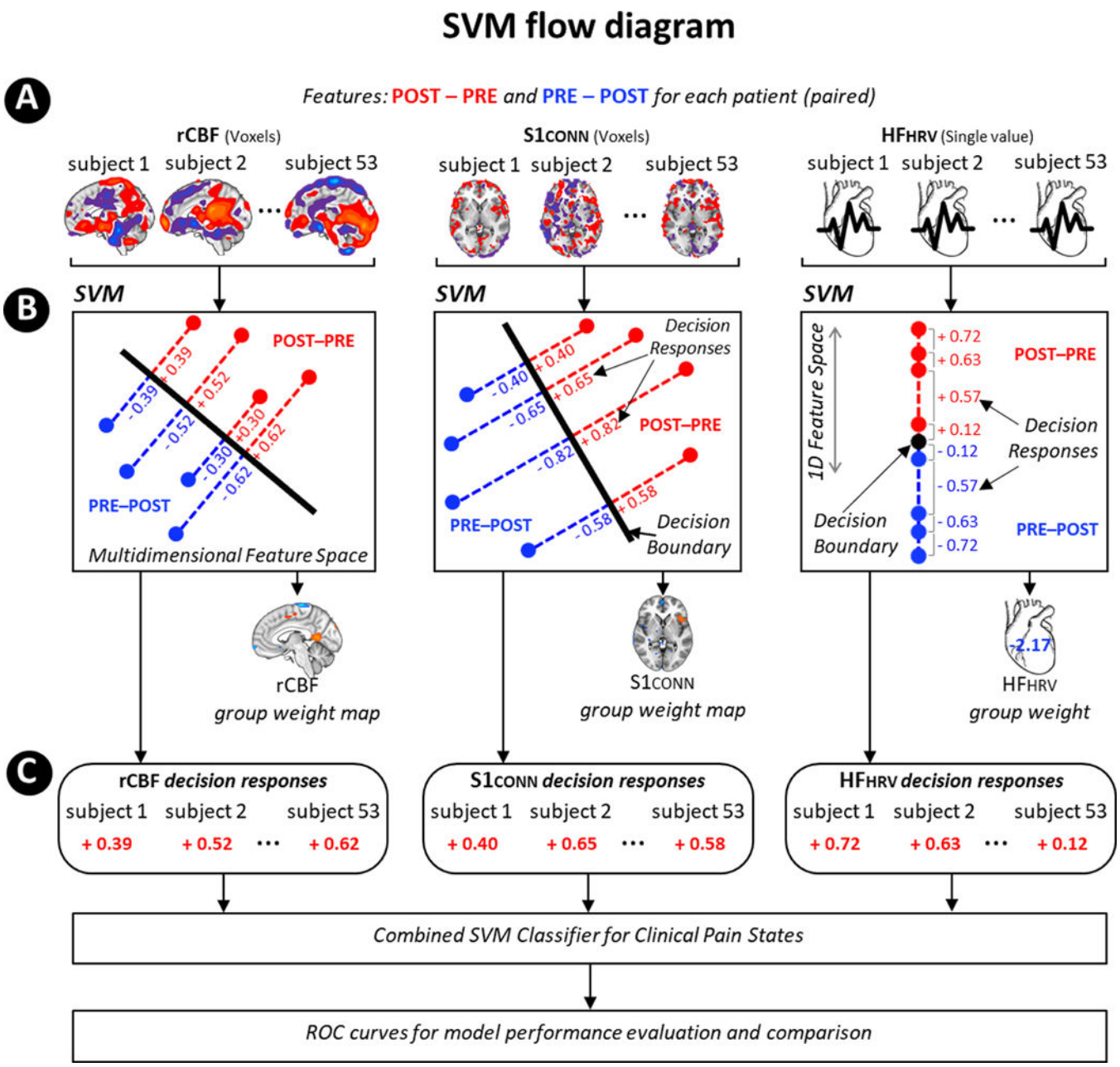

Figure 1. Classification of within-patient clinical pain states using a support vector machine (SVM).

(A) Each patient provided rCBF voxels, $S1_{CONN}$ voxels, and HF_{HRV} values as multimodal input features to the SVM algorithm. (B) The paired classifier discriminated between POST-PRE and PRE-POST in feature space by fitting a decision boundary that maximally separates them, for each modality. This SVM procedure produces (C) decision responses and weights for each modality. The decision responses for each modality were combined for a synergistic classifier of clinical pain states. The weights for each modality were used in the SVR analysis (see Figure 2). N.b. rCBF: regional cerebral blood flow, $S1_{CONN}$: $S1_{back}$-connectivity, HF_{HRV}: high frequency heart rate variability power, PRE: pre-maneuver, POST: post-maneuver.

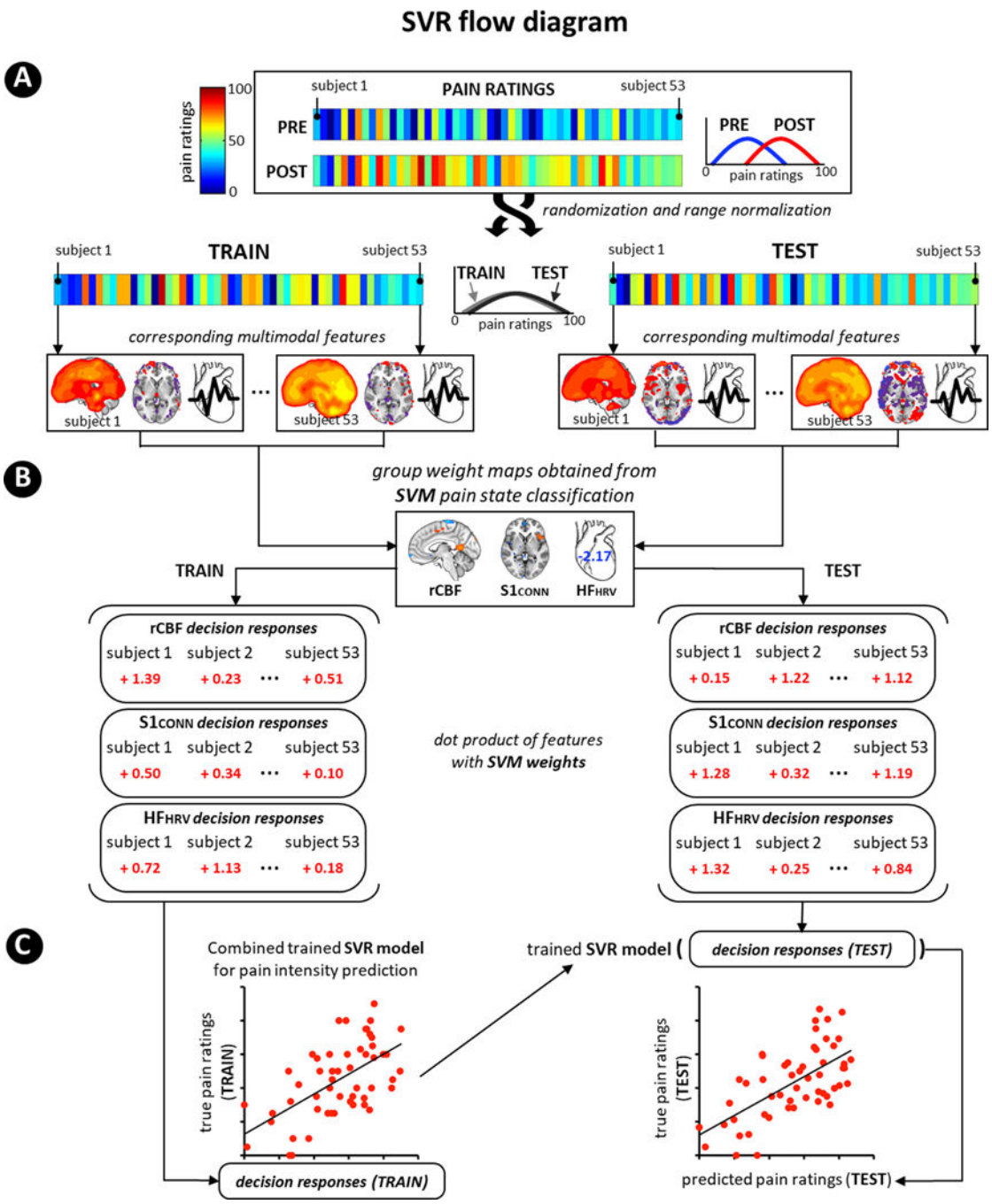

Figure 2. Prediction of between-subject clinical pain intensity using support vector regression (SVR).

(A) Clinical pain ratings for each patient (*N*=53) were randomized, and equally allocated into TRAIN and TEST datasets (providing total effective N=106). This randomization into TRAIN and TEST equalized the range of pain ratings, previously found to be discrepant between PRE and POST. Corresponding multimodal features for each clinical pain intensity timepoint were taken, and (B) decision responses were calculated using a dot product between multimodal features and corresponding SVM classification group weights, resulting in decision responses for each modality. (C) The decision responses for TRAIN and

corresponding clinical pain ratings were used to build an SVR model. The trained SVR model was then applied to decision responses from TEST, to produce an output of predicted pain ratings. The true (TEST) and predicted pain ratings were plotted and a Pearson's correlation coefficient was computed to evaluate model performance. N.b. rCBF: regional cerebral blood flow, $S1_{CONN}$: $S1_{back}$-connectivity, HF_{HRV}: high frequency heart rate variability power, PRE: pre-maneuver, POST: post-maneuver.

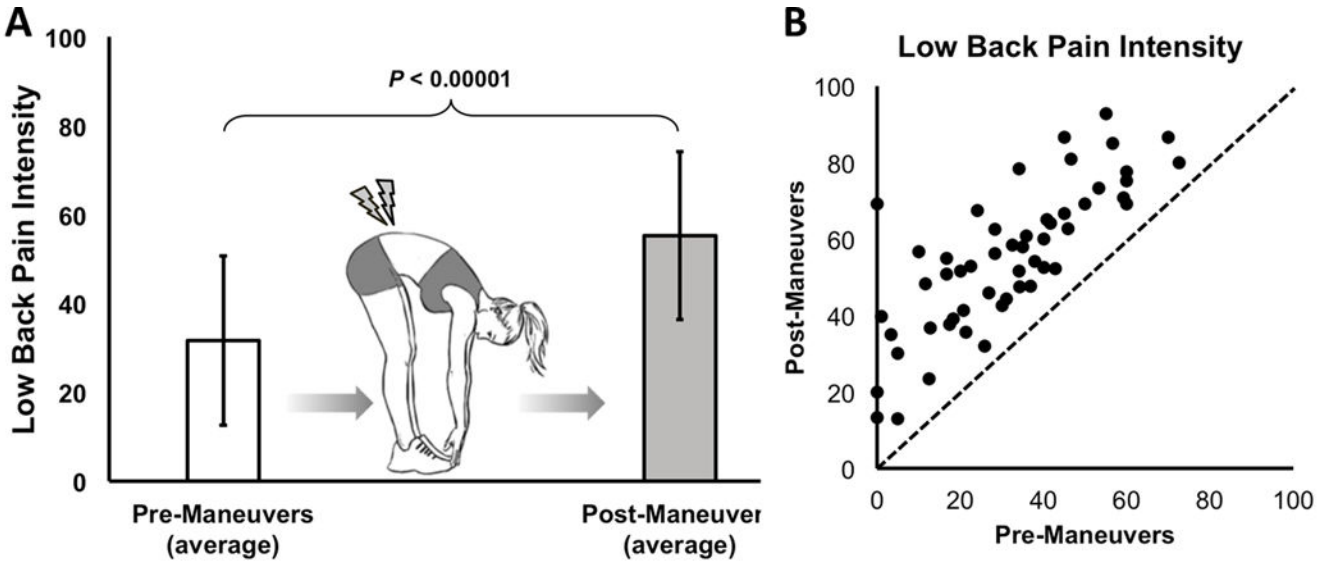

Figure 3.

Clinical pain intensity changes due to physical maneuvers. (A) Individually customized physical maneuvers significantly exacerbated low back pain levels in cLBP patients (*N*=53). (B) Patients reported a wide range of baseline low back pain levels (pre-maneuvers) and after maneuvers, all included patients reported increased pain levels (post-maneuvers), which were maintained throughout the duration of the post-maneuver scans. N.b. Bar plots in (A) show mean±SD. Each data point in (B) represents an individual patient.

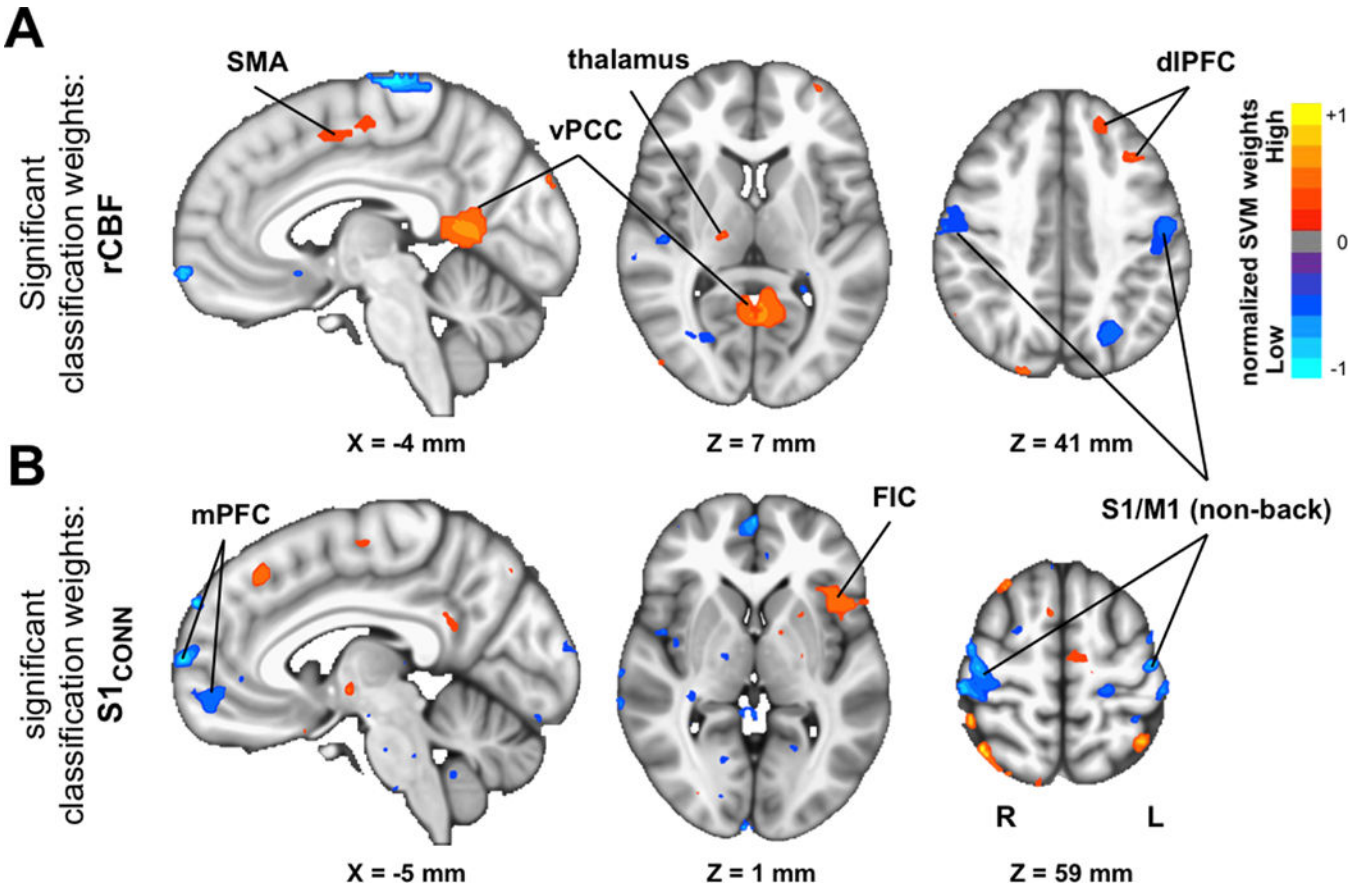

Figure 4.

Brain features significantly contributing to within-patient classification of lower- and higher-clinical pain intensity states. Paired-SVM classification weight maps for rCBF (A) and $S1_{CONN}$ (B) were thresholded (permutation analysis with N=5000, P<0.01) for visualization. N.b. rCBF: regional cerebral blood flow, $S1_{CONN}$: S1-connectivity, SMA: supplementary motor area, vPCC: ventral posterior cingulate cortex, dlPFC: dorsolateral prefrontal cortex, S1: primary somatosensory cortex, M1: primary motor cortex, mPFC: medial prefrontal cortex, FIC: frontoinsular cortex, R: right hemisphere, L: left hemisphere.

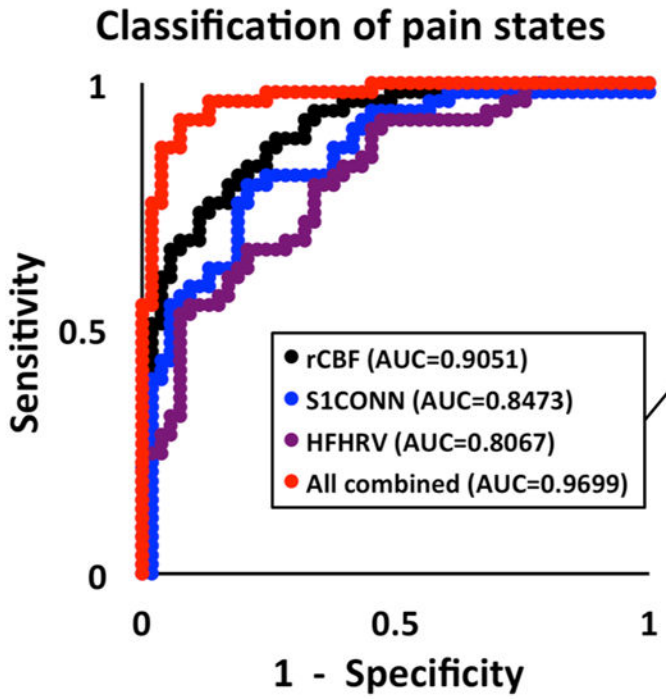

Parameters	Accuracy (%)	AUC
rCBF	81.13	0.9051
$S1_{CONN}$	79.24	0.8473
HF_{HRV}	67.92	0.8067
rCBF + $S1_{CONN}$	90.56	0.9633
rCBF + HF_{HRV}	86.79	0.922
$S1_{CONN}$ + HF_{HRV}	81.13	0.8902
All Combined	92.45	0.9699

Figure 5.

Receiver operating characteristic (ROC) curves demonstrated superiority of combined parameter classification of relatively higher versus lower clinical pain intensity states. Comparison of individual-parameter versus combined-parameter classification performance using paired-SVM demonstrated most improved performance for the combined 3-parameter model. N.b. for a paired-SVM approach, sensitivity, specificity, and precision are identical to accuracy. rCBF: regional cerebral blood flow, $S1_{CONN}$: S1-connectivity, HF_{HRV}: high frequency power of heart rate variability, AUC: area under the curve.

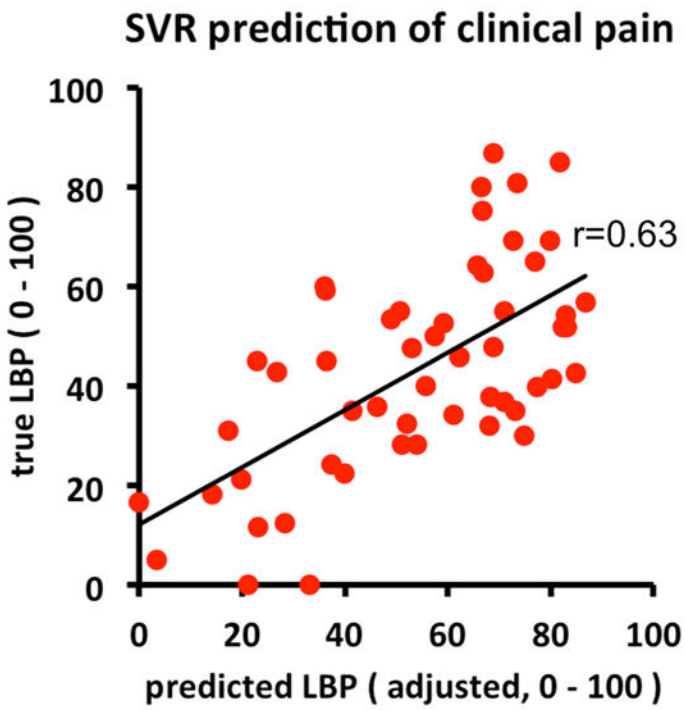

Figure 6.

Prediction of clinical low back pain ratings across cLBP patients using all multimodal parameters. True LBP plotted against Predicted LBP from SVR results demonstrated that our model was successfully able to predict between-subject clinical pain intensity ratings for both a training (TRAIN, N=53, r=0.52) and independent testing dataset (TEST, N=53, r=0.63, shown above).

Table 1.

Demographic and clinical characteristics of cLBP patients.

Measures (cLBP, *N*=53)	**Values/scores**
Age (years old)	37.4 ± 11.3
Sex (male/female)	20/33
Pain duration (years)	7.6 ± 7.4
% using opioids	5.70%
BDI	5.6 ± 6.3
BPSD	8.3 ± 4.1
PROMIS-Physical function (T-score)	42.5 ± 4.0
PROMIS-Pain interference (T-score)	58.1 ± 5.5
PCS	11.7 ± 8.4
Back pain bothersomeness	5.0 ± 1.6

cLBP: chronic low back pain, BDI: Beck Depression Inventory II (0–63 scale), BPSD: Back Pain Specific Disability (0–10 scale), PROMIS: Patient-Reported Outcomes Measurement Information System, PCS: Pain Catastrophizing Scale. Back Pain Bothersomeness was collected on a VAS scale (0: “not at all bothersome”, 10: “extremely bothersome”). Data are shown as mean±SD.